Hindawi
Advances in Civil Engineering
Volume 2019, Article ID 2054938, 12 pages
https://doi.org/10.1155/2019/2054938

Research Article

Influence of Fault on the Surrounding Rock Stability for a Mining Tunnel: Distance and Tectonic Stress

Zhiqiang Zhang,[1] **Fangfang Chen**,[2] **Ning Li**,[1] **and Mingming He**[1]

[1]*Institute of Geotechnical Engineering, Xi'an University of Technology, Xi'an 710048, China*
[2]*School of Architecture and Civil Engineering, Xi'an University of Science and Technology, Xi'an 710056, China*

Correspondence should be addressed to Zhiqiang Zhang; zhangzq87@xaut.edu.cn

Received 7 March 2019; Revised 29 May 2019; Accepted 15 June 2019; Published 18 July 2019

Academic Editor: Hossein Moayedi

Stability of surrounding rock mass and safety of supporting system in mining tunnel are always dominated by fault near excavation limit. The influence degree of the fault varies significantly under different fault distances to mining tunnel and initial stresses condition. In this paper, a series of numerical experiments are conducted to study the displacement, stress, and plastic region in surrounding rock mass. The stress characteristics in sprayed concrete layer are analyzed to study the influence of the fault distance on excavation limit and the initial stress in ground. The fault distance is defined geometrically by a mutual perpendicular line between the excavation limit and fault line nearest to the mining tunnel to quantify the influence. In order to simulate fault specialty reasonably, an interface model based on the theory of cohesive joint element is proposed in the numerical experiment model. Some other disciplinary and quantificational regularities about the influence of the fault distance and tectonic stress are summarized based on the numerical results. The results show that there is a critical distance to judge whether a fault has a prominent influence to mining tunnel. The critical distance depends on the quality of mining tunnel surrounding rock mass, initial stress, and the degree of excavation limit curvature. With the increase of lateral stress coefficient, the vertical displacement at crown decreases, but the horizontal displacement increases in the both right and left sidewalls.

1. Introduction

Fault always provokes surrounding rock stability issues during construction and operation period of mining tunnel. Hence, increasing attention has been paid to influence of the fault on the stability of surrounding rock mass of mining tunnel [1]. Scientific reports on the collapse of tunnel surrounding rock demonstrate that the location of the fault relative to mining tunnel and the mechanical properties of the fault always control the failure pattern of the surrounding rock and the supporting system [2]. Therefore, a whole and comprehensive understanding of the influence of the fault on the tunnel surrounding rock stability is beneficial to the safety of construction and operation of the mining tunnel engineering.

Fault in mining tunnel surrounding rock mass behaves differently in different conditions of initial ground stress, rock mass quality, fault thickness, distance, and location to mining tunnel. The influence of the rock mass quality, the fault thickness, and the location to mining tunnel on the stress and plastic zone in tunnel surrounding rock mass and the stress in the sprayed concrete lining had been studied by numerical approach [3]. However, there are few studies about the distance from fault line to the mining tunnel excavation limit and the initial ground stress that are also crucial factors to fault behaviors. This paper investigated and discussed that the effect of the fault distance and the initial ground stress in strata on the stability of mining tunnel surrounding rock mass and the safety of supporting system.

Many different methods are utilized to explore the influence of the fault on the stability of mining tunnel surrounding rock mass. Lots of results have been obtained in the last two decades. In early times, scaled model experiments were carried out to study the stability of the ground and the roof support with changing in the cross section of mining tunnel by considering the fault near mining tunnel

[4]. The scaled method also was used to study the influence of the fault orientation on the stability of mining tunnel. The experiment results show that the curvature of mining tunnel excavation limit affects heavily the deformation and the stress of surrounding rock mass [5]. The displacement and the area of the plastic region decrease with the increasing of the fault distance, and the displacement of rock mass in crown is larger under the condition when the fault locates across the upper part of the mining tunnel than that in the case when the fault locates at the left sidewall of the mining tunnel [6]. An experiment simulating normal fault displacements with different dip angles was performed to study the rupture propagation in strata and the mining tunnel failure under fault displacement [7]. The test results show that more than one strata rupture appears when the normal fault moves and at least one rupture reaches the ground surface as the vertical fault dislocation is approximately 4.4% of the covering depth.

In recent years, lots of efforts are focused on studying the mechanism of the influence of the fault on the mining tunnel surrounding rock mass and supporting system and how to reduce and control the influence. Since the 1980s, tendency of using numerical method is becoming stronger in academe and engineering scopes due to its repeatability and economic efficiency [8]. The numerical research on the fault influence in the mining shaft show that the area of the tension zone around shaft has a good agreement with the results recorded in the construction site [9]. The rock displacement and plastic region around the mining tunnel are considered index for evaluating the stability of mining tunnel surrounding rock mass [10]. The fault close to mining tunnel always has predominant influence on mining tunnel stability, and the influence becomes stronger as the fault locates closer to the tunnel. The distance between the fault and mining tunnel excavation limit is one of the key factors influencing the stability of mining tunnel [11]. In this paper, the fault distance is defined based on the geometries of two kinds of mining tunnels with different cross section shapes. The influence of the fault distance on the stability of mining tunnel surrounding rock is studied by means of numerical experiment.

The ground stress in rock stratum has a large variation under different tectonic structures. The initial ground stress is one of the important environmental influencing factors on the behaviors of the fault close to mining tunnel [12]. The fault close to mining tunnel always causes the diverse deformation or second stress field in the surrounding rock mass under the initial ground stress with the different lateral stress coefficients, especially under the initial stress with high tectonic stress [13, 14]. The influence of initial ground stress on the stability of mining tunnel surrounding rock is also investigated by the numerical experiment in this paper.

In FEM numerical experiment, the fault modelling is the most critical factor to achieve the reasonable results. In this paper, to simulate the fault accurately, the fault model is established by the cohesive joint (COJO) element embedded in the FEM code named FINAL from Austria [15]. There are three main numerical models for the fault, which are the Goodman model, Desai new element, and COJO element. The Goodman model based on mechanics nature of jointed rock was proposed by prof. Goodman in 1970s, which is one of the most popular models in rock mechanics field [16]. In 1980s, a thin layer element for interface and joint was created by Desai et al. [17]. In 1990s, COJO element, a featured discontinuity model, was suggested based on Coundal's interface model, including only friction coefficient, cohesion, and tensile strength as input mechanical parameters [18]. The original COJO element was applied to simulate the fault around mining tunnel. In this paper, an interface model based on the theory of COJO element is proposed in the numerical experiment model to study the displacement, stress, and plastic region in the surrounding rock mass. The stress characteristics in the sprayed concrete layer are analyzed to study the influence of the fault distance on the excavation limit and the initial stress in ground. The fault distance is defined geometrically by a mutual perpendicular line between the excavation limit and fault line nearest to mining tunnel to quantify the influence.

2. Fault Distance Definition and Initial Stress in Stratum

2.1. Fault Distance Definition. Figure 1 shows a fault locating near to a mining tunnel with cross section of horseshoe shape (Figure 1(a)) or rectangular conduit with circular upper wall (Figure 1(b)). In the figure, the fault was drafted approximately by a straight line with a width. The marks A to F divide the excavation limit into 6 segments, named segments AB, BC, CD, DE, EF, and FA. The segment CD is called the crown segment. Segments BC and DE are shoulder segments near both sides of the crown segment. Segments AB and EF are left and right sidewall segments, respectively. Segment FA is the bottom segment. The definition of the fault location around the mining tunnel is presented in detail in [3]. The definition of the fault distance (i.e., the distance between the fault and the mining tunnel) will be discussed as follows. A series of mutual perpendicular lines can be drawn between the mining tunnel excavation limit and the fault line in Figure 1. Among these mutual perpendicular lines, the shortest line MN represents the fault distance.

2.2. Initial Stress in Stratum. The complexity of the initial ground stress has been recognized in underground engineering. Furthermore, the initial ground stress has significant effect on the stability of mining tunnel surrounding rock mass [19], especially the surrounding rock with fault [20]. In common background, the vertical stress σ_v and the horizontal stress σ_h in rock stratum can be calculated by the following [21]:

$$\begin{aligned} \sigma_v &= \gamma H, \\ \sigma_h &= k_0 \gamma H, \end{aligned} \tag{1}$$

where H is the depth from the ground surface, γ is the average unit weight of the rock layer, and k_0 is the lateral stress coefficient.

For a specific point in stratum, the vertical stress always can be expressed by equation (1) because the average unit

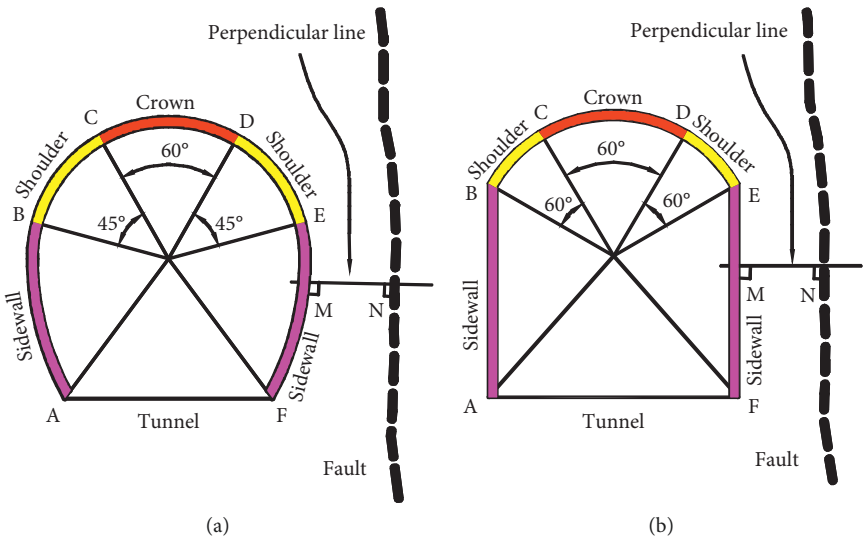

Figure 1: Mining tunnel, fault, and fault distance: (a) mining tunnel with the shape of horseshoe; (b) mining tunnel with shape rectangular conduit with circular upper wall.

weight of rock mass γ and the depth from ground surface H can be obtained easily and accurately. But the lateral stress coefficient k_0 that varies dramatically with geologic structure is difficult to be gained in construction site.

3. Modelling, Studying Case, and Concerning Point

3.1. Numerical Modelling of Fault. Remarkable discontinuity is the main property for the fault near the mining tunnel. A numerical method that can produce equivalently discontinuity phenomena is reasonable to reach the aim to simulate the fault realistically. An interface model can be used to produce discontinuity, such as the Goodman element [22], Desai new element [17], and COJO element [18]. With an interface model, the fault in the numerical model can behave with discontinuous displacement and stress field under the tensile and shear stress.

The COJO element based on Coundal's interface model is selected to simulate the fault in this paper. COJO element has four nodes, two of which are used to define force and displacement and other two are used to define element direction. All the nodes of the COJO element are the solid elements; thus, there is not any extra node to assemble the COJO elements shown in Figure 2.

In Figure 2, a fault connects rock parts A and B, which are meshed by solid triangle element with six nodes. The nodes i and j are real nodes for monitoring displacements of unknowns, the nodes k and l are imaginative nodes for showing the direction of COJO element, the local direction n is normal to fault, the local direction s is tangent to fault, the σ is the normal force on fault, and the τ is the tangent force on fault.

In COJO element, the contact force and the displacement of the node are chosen as additional unknowns in the governing equation to overcome the disadvantage of input parameters for traditional interface element. The relationship between contact stress on the node and node load is shown in equation (2).

$$\mathbf{C}^T \int N^{\mathrm{T}} N \, d\Gamma \Delta\sigma = \Delta\mathbf{F}, \tag{2}$$

where $\mathbf{C}$ is the transformation matrix between contact stress and node load, N is the shape function matrix, and $\Delta\sigma$ and $\Delta\mathbf{F}$ are contact stress and incremental node load, respectively.

Equation (3) is the equation of COJO element to geometry and constraint:

$$\left\{ \mathbf{C}^* \quad \mathbf{R} \right\} \begin{Bmatrix} \Delta\mathbf{a} \\ \Delta\sigma \end{Bmatrix} = \mathbf{a}^*, \tag{3}$$

where $\mathbf{R}$ is the diagonal matrix, $\Delta\mathbf{a}$ is the incremental node displacement, and $\mathbf{a}^*$ is the constraint load vector related to the status of COJO element.

Making a combination of the equations (2) and (3), the element stiffness matrix and the element load vector are obtained by the following equation:

$$\begin{bmatrix} \mathbf{0} & \mathbf{C}^{\mathrm{T}} S \\ \mathbf{C}^* & \mathbf{R} \end{bmatrix} \begin{Bmatrix} \Delta\mathbf{a} \\ \Delta\sigma \end{Bmatrix} = \begin{Bmatrix} \Delta\mathbf{F} \\ \mathbf{a}^* \end{Bmatrix}, \tag{4}$$

$K_{\mathrm{c}} = \begin{bmatrix} \mathbf{0} & \mathbf{C}^{\mathrm{T}} S \\ \mathbf{C}^* & \mathbf{R} \end{bmatrix}$, and $f_{\mathrm{c}} = \begin{Bmatrix} \Delta\mathbf{F} \\ \mathbf{a}^* \end{Bmatrix}$, where K_{c} and f_{c} are the element stiffness matrix and element load vector, respectively.

3.2. General Information on Mining Tunnel. In mining tunnel engineering, the faults near mining tunnel crown and sidewall always have greater influence than that located elsewhere such as the bottom zone. Therefore, the faults near the mining tunnel crown and sidewall are chosen to investigate the influence of the fault distance and the tectonic stress on the stability of mining tunnel surrounding rock mass.

A typical mining tunnel with the shape of rectangular conduit and circular upper wall, as shown in Figure 3(a), is

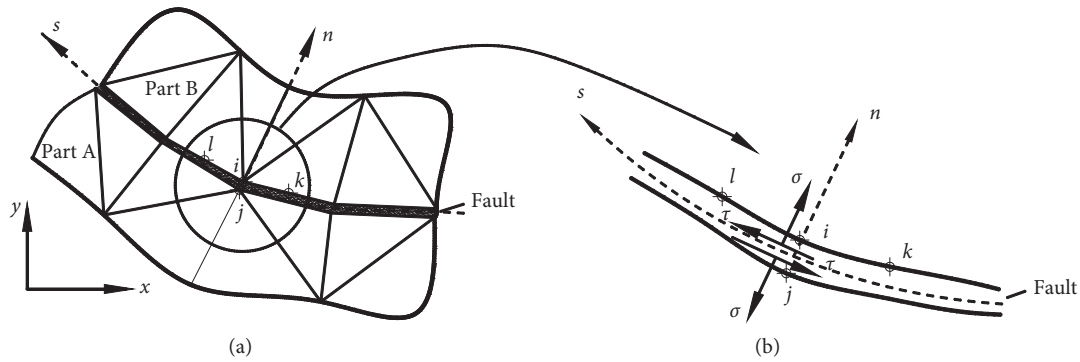

Figure 2: COJO element along the interface between two rock parts.

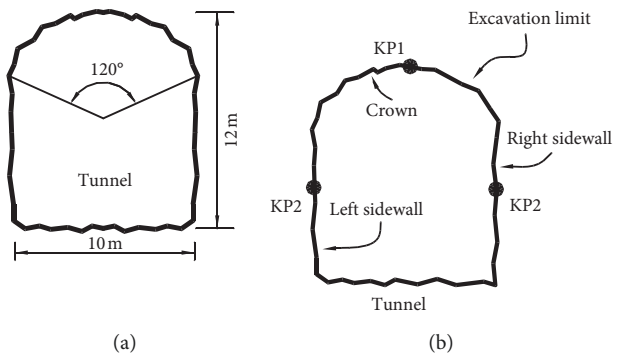

Figure 3: Geometry of mining tunnel and concerning point. (a) Geometry of mining tunnel; (b) concerning point.

selected as the model mining tunnel in this paper. The mining tunnel has the height of 12.0 m, the span of 10.0 m, the crown angle of 120°, and overburden of 100.0 m. The fault in surrounding rock mass locates near the mining tunnel crown or sidewall. After the excavation, the mining tunnel is supported by the shotcrete layer with a thickness of 10 cm.

The surrounding rock mass of the mode mining tunnel is classified in graded III according to the *Chinese Code for Engineering Geological Investigation of Water Resources and Hydropower Engineering,* which is considered as an idealized elastoplastic material followed the Mohr–Coulomb yield criterion. The mining tunnel supporting system is treated as elastic material. The mechanical parameters of rock mass and supporting material are listed in Table 1.

3.3. Studying Case. In the geological condition, the fault distance has a range of centimetres to kilometres. However, in practical mining tunnel engineering, only the fault close to mining tunnel affects apparently the stability of surrounding rock mass and support system. Five tunnel cases with different fault distances are discussed in this paper, which were 0.2 spans, 0.5 spans, 1.0 span, 2.0 spans, and 3.0 spans. The layout of the crown and sidewall faults with different fault distances is presented in Figure 4.

The lateral stress coefficient k_0 in stratum with tectonic stress is in the range from 0.2 to 10.0. In most underground engineering, the lateral stress coefficient has the range concentrated from 0.3 to 5.0 [23]. In this paper the main range of 1.0 to 3.0 is chosen to analyze the influence of ground stress. Five lateral stress coefficients representing five ground stress conditions are set in numerical experiment, which are 0.38, 1.0, 1.5, 2.0, and 3.0. The value of 0.38 represents the initial stress dominated by gravity. All the lateral stress coefficients are shown in Figure 5.

3.4. Influence Index. For a mining tunnel, displacement, stress, tensile stress zone, and plastic zone are key factors to evaluate the stability of surrounding rock mass. For shotcrete layer, the stress is key factor to safety. Above indexes will be discussed according to results of numerical experiment.

In the mining tunnel with the shape of rectangular conduit and circular upper wall, some points are treated as the key points to the stability evaluation of surrounding rock mass, such as the top point of crown (KP1) and the middle points of sidewall (KP2 and KP3), as shown in Figure 3(b). The displacements and stresses of the three points will be further discussed.

A ratio λ_d named displacement ratio is used to identify the influence level of the fault on the deformation. λ_d is the ratio of the displacement of a point on the tunnel excavation limit under the case with fault in surrounding rock to that under the case without fault, as shown in equation (5).

$$\lambda_d = \frac{d_f}{d_0}, \tag{5}$$

where d_f and d_0 are the displacements of the point on the mining tunnel excavation limit under the cases with and without fault in surrounding rock, respectively.

In the same way, the stress ratio λ_s can also be calculated as follows:

$$\lambda_s = \frac{s_f}{s_0}, \tag{6}$$

where s_f and s_0 are the stresses at the point on the mining tunnel excavation limit under the cases with and without fault in surrounding rock, respectively.

Table 1: Mechanical parameter for rock mass and mining tunnel supporting material.

Material	Deformation modulus (GPa)	Possion's ratio	Cohesion (MPa)	Frictional angle (°)	Tensile strength (MPa)	Unit weight (kN/m^3)
Rock mass (graded III)	6.0	0.28	1.2	40.0	1.0	26.0
Fault and its filling	0.1	0.40	0.6	23.0	0.0	23.0
Shotcrete	21.0	0.18	—	—	1.2	24.0

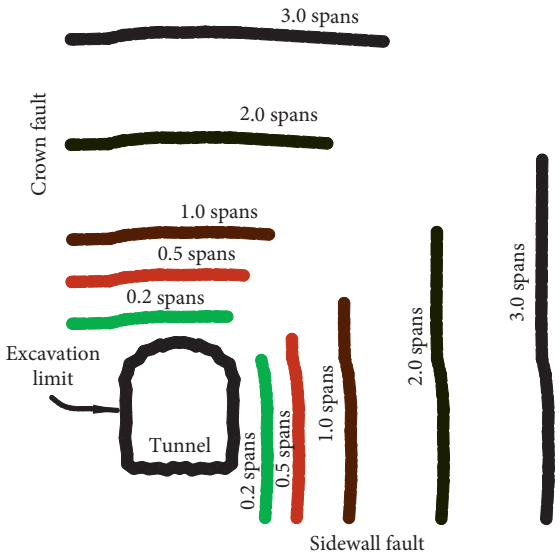

Figure 4: Crown and sidewall faults with different distances from tunnel limit.

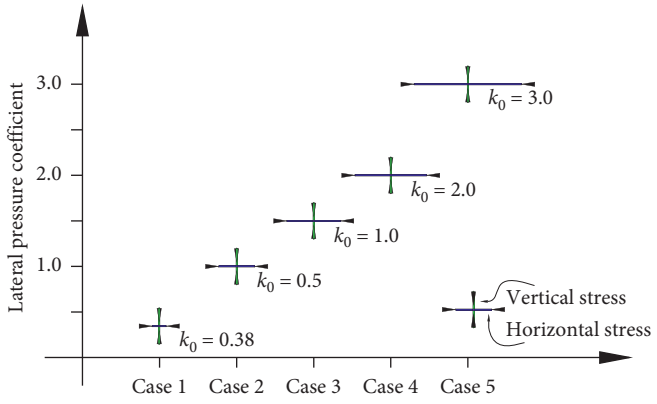

Figure 5: Lateral stress coefficient for five cases.

4. Influence of Fault Distance

4.1. Displacement and Displacement Field. The displacement ratios of the points KP1, KP2, and KP3 (shown in Figure 3(b)) on the mining tunnel excavation limit are presented in Figure 6. Note that the displacement of the middle point in the left sidewall equals approximately to that in the right sidewall for each associated case due to symmetry. As shown in Figure 6, with the decrease of the fault distance, the displacement at top point of the crown increases, whereas the displacements at the both sidewalls have a decreasing tendency.

The displacement at the top of the tunnel crown of the case without fault is 6.13 mm, whereas the displacements at the same point of the three cases with fault distance of 1.0 span, 0.5 spans and 0.2 spans are 7.67 mm, 11.43 mm and 24.06 mm, respectively. Comparing with the displacement of the case without fault, the increasing percentages of the three cases are 25.0%, 86.5%, and 292.5%, respectively. The fault with 0.2 spans to the mining tunnel excavation limit will provoke a dramatic leap in rock mass displacement, even a collapse around the crown.

The surrounding rock mass can divided into two parts by fault: (1) the part between the excavation limit and the fault and (2) the part beyond the fault. When the fault is forced to be open by excavation load, the part between the excavation limit and the fault will detach from the whole surrounding rock mass, bearing entire excavation load alone. The closer is the fault to the mining tunnel excavation limit, the easier is the fault forced to be open, causing greater deformation in the crown rock.

The surrounding rock displacement decreases with the increasing of the fault distance. For example, for the case with the fault distance of 1.0 span, the horizontal displacement is 1.39 mm, whereas the rock displacement decreases to 0.95 mm when the fault distance goes down to 0.2 spans. Comparing with the surrounding rock displacement in the no fault case, the sidewall displacements in the cases with the fault distances of 1.0 span, 0.5 spans, and 0.2 spans decrease by 14.3%, 28.6%, and 42.9%, respectively. The main reason of the decrease in the deformation of surrounding rock is that the more surrounding rock mass near the mining tunnel crown goes down as the fault distance decreases. The downward movement in the crown rock prevents the surrounding rock mass in the sidewall from moving towards the inner section of mining tunnel. Hence, the rock displacements in sidewall go down with the decrease of the fault distance.

The displacement vector fields under four different conditions of fault distance are shown in Figure 7. The displacements of the surrounding rock mass between the fault and the excavation limit have an increasing trend as the fault moves from deep rock mass to excavation limit, whereas the displacements of the surrounding rock mass beyond the fault have a decreasing tendency. For the cases with fault distance of 0.2 spans and 0.5 spans, there are striking displacements in the zone between fault and excavation limit, whereas the displacements in the zone beyond the fault are too small to be identified due to the fault opening under the larger excavation load. When the fault distance is greater than 1.0 span, obvious displacements occur in the rock mass beyond the fault.

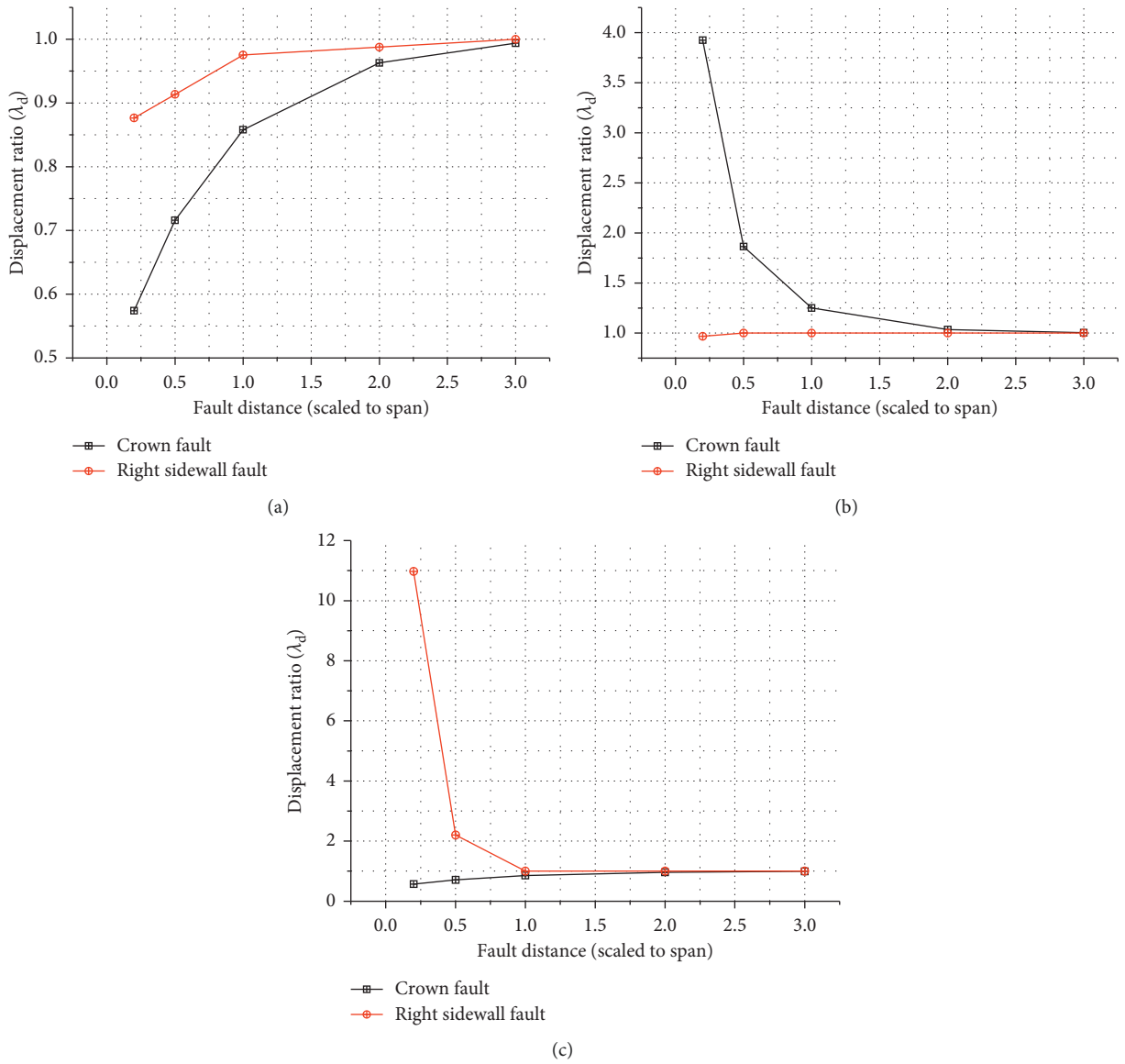

Figure 6: The displacement ratio vs. fault distance: (a) middle point of left sidewall; (b) top of crown; (c) middle point of right sidewall.

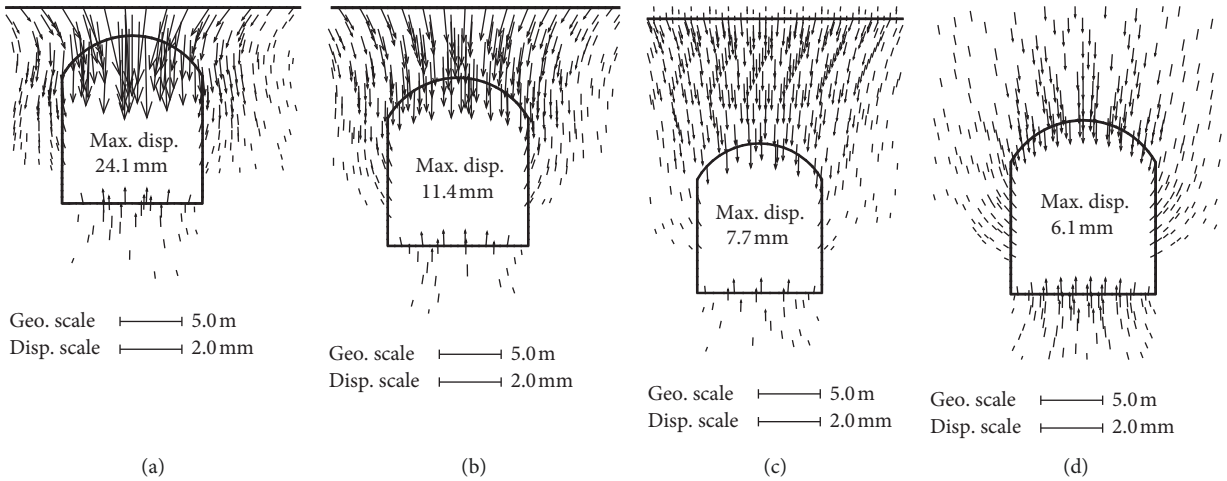

Figure 7: Displacement vector fields of the surrounding rock mass with different fault distance cases: (a) 0.2 spans; (b) 0.5 spans; (c) 1.0 span; (d) no fault.

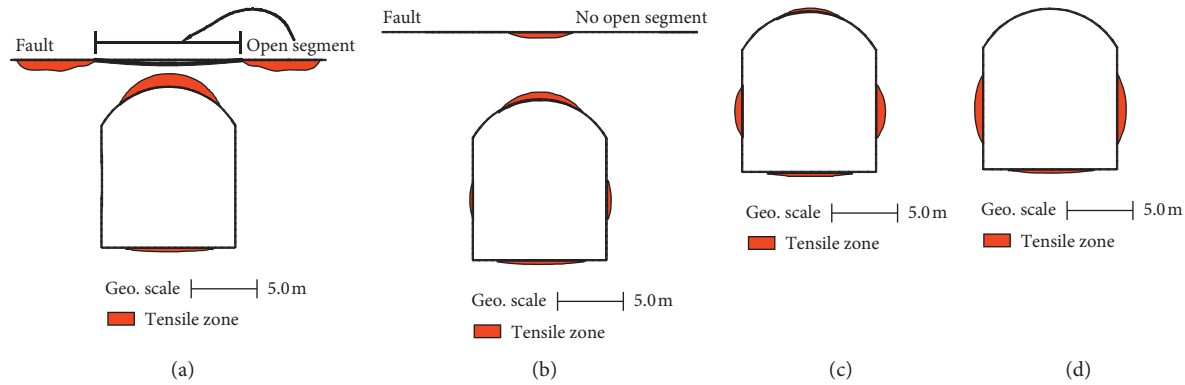

Figure 8: The tensile stress area of the surrounding rock mass: (a) 0.2 spans; (b) 0.5 spans; (c) 1.0 span; (d) no fault.

The maximum displacements in the four cases in Figure 7 are 24.1 mm, 11.4 mm, 7.7 mm and the 6.1 mm, respectively. The fault located near the excavation limit has an obvious barrier effect on displacement field of the surrounding rock mass. This barrier effect will prevent the excavation load from transferring from the rock mass between the excavation limit and the fault to that beyond the fault, making the surrounding rock mass between the fault and excavation limit overburden more loads, even the entire excavation load. As a result, the displacement of the rock mass between the fault and the excavation limit increases dramatically, eventually leading to the instability of the surrounding rock.

4.2. Stress and the Tensile Stress Area of Surrounding Rockmass. Stress or stress field of mining tunnel surrounding rock mass, especially tensile stress, are the other evaluation indexes for the stability of mining tunnel surrounding rock mass. Figure 8 shows the stress vector fields of the four cases under different conditions of fault distance. The tensile stress area near the mining tunnel excavation limit has a decreasing trend as the fault moves from the excavation limit to deep surrounding rock mass. When the fault distance is 0.2 spans, the tensile stress occurs massively in the crown zone and both sides of surrounding rock mass under the fault. For the case with fault distance of 0.5 spans, the tensile stress appears mainly in the core crown and slightly in one side of the fault. When the fault distance reaches 1.0 span, both the value and the area of tensile stress are small. For the case without fault, the situation of the surrounding rock mass is very well.

According to the analysis of tensile stress datum, the value and area of tensile stress increase with the decreasing of fault distance. The fault distance larger than 1.0 span affects the value and area of the tensile stress in the surrounding rock mass of mining tunnel significantly, which can be considered as the critical distance on evaluating the fault influence.

4.3. Plastic Region of Surrounding Rockmass. The plastic regions in the surrounding rock mass under different fault distances are presented in Figure 9. Besides fault distance, the distribution of plastic region is affected by the mining tunnel shape [24]. For the mining tunnel with shape of rectangular conduit and circular upper wall, the plastic region occurs around the four corners under the condition without fault as shown in Figure 9(d). For the cases with fault, the plastic region in the surrounding rock mass increases obviously as shown in Figures 9(a)–9(c).

For the case with a fault distance of 1.0 span (see Figure 9(c)), the plastic region expands along the excavation limit from the four corners to the middle zone of both sides of sidewall and the top zone of the crown, mainly develops in both sidewalls zone. For the case with fault distance of 0.5 spans (see Figure 9(b)), both sidewall parts are covered with plastic regions, and the maximum depth of the plastic region is about 0.1 spans. For the case with the smallest fault distance of 0.2 spans in this paper (see Figure 9(a)), the plastic zone covers the surrounding rock mass all around the mining tunnel, and the maximum depth is 0.4-0.5 times the mining tunnel span. In Figure 9, the number of the plastic elements of the case with fault distances of 0.2 spans is approximately 5 times that of the case with no fault, and 3.0 times and 1.5 times that of the cases with fault distances of 0.5 and 1.0 spans, respectively.

4.4. Inner Force and Stress in Sprayed Concrete Layer. Figure 10 presents the distributions and the values of the axial forces in the sprayed concrete layers under different fault distances. For the cases with the fault distances of 0.2 spans and 0.5 spans, the axial forces are tensile, with the maximum values of 356.9 kN and 54.0 kN, respectively. For the case with the fault distance of 1.0 span, the axial force in crown zone changes from tensile force to compressive force, and the maximum value are 38.8 kN. The crown fault near the excavation limit can change the compressive axial force into tensile axial force in crown segment, so long as the fault distance is enough small. Accordingly, fault has an effect on the distribution of the axial force in sprayed concrete layer. The axial force in some parts of sprayed concrete layer increases, and in some parts decreases as the fault moves the from excavation limit (0.2 span) to deep surrounding rock mass (no fault).

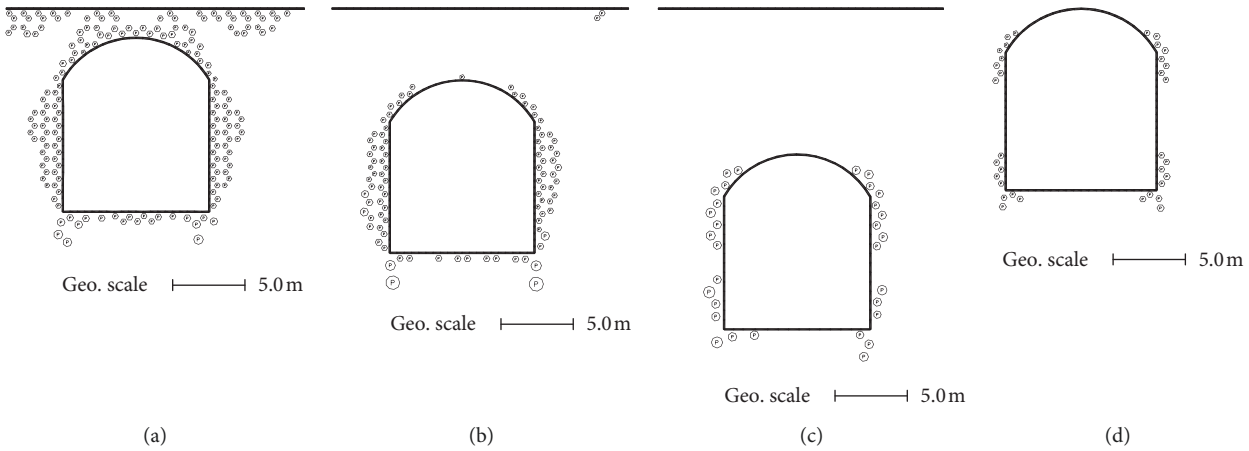

Figure 9: Plastic region of the surrounding rock mass with different fault distance cases: (a) 0.2 spans; (b) 0.5 spans; (c) 1.0 span; (d) no fault.

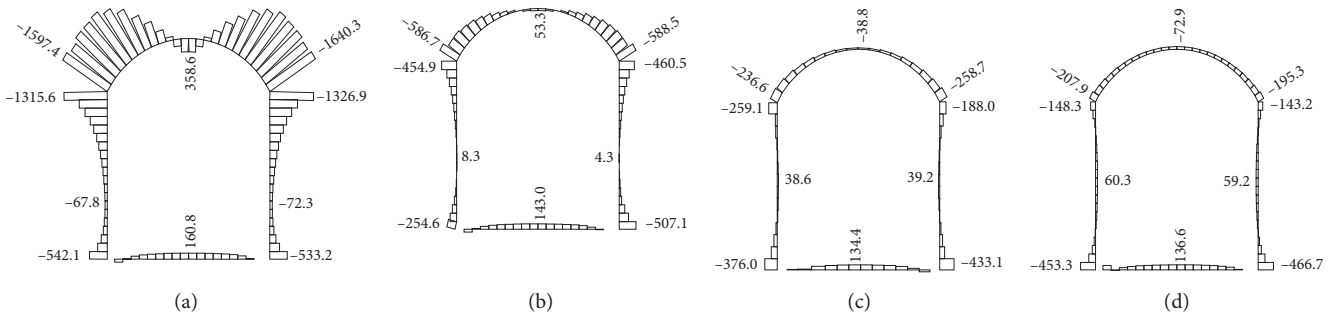

Figure 10: Diagram of axial forces in sprayed concrete layer with different fault distance cases: (a) 0.2 spans; (b) 0.5 spans; (c) 1.0 span; (d) no fault.

The featured stress in sprayed concrete layer, such as the stressed at the middle points of both sides of sidewall and the top point at the crown are list in Table 2. The stress in sprayed concrete layer is influenced dramatically by the fault near the mining tunnel excavation limit. The featured stress in sprayed concrete layer at mining tunnel crown changes from compressive stress to tensile stress as the fault moves from deep surrounding rock mass (no fault) to the excavation limit (0.2 span). On the contrary, the stress in sprayed concrete layer at the middle point of sidewall changes from tensile stress to compressive stress. When the crown fault locates about 1.0 span to the excavation limit, the stress in the sprayed concrete layer is about 30–45% of the stress in the case without fault. When the fault distance is 0.2 spans, the stress in the sprayed concrete layer at the mining tunnel crown is larger than the tensile strength of the sprayed concrete and about 5 times that in the case without fault. The stress in the sprayed concrete layer at the midpoint of sidewall is about 3 times that in the case without case.

Table 2: Max stress and min stress in sprayed concrete layer under different cases.

Distance	Middle point of left sidewall		Top point of crown		Middle point of right sidewall	
	σ_{max}	σ_{min}	σ_{max}	σ_{min}	σ_{max}	σ_{min}
No fault	0.62	0.59	−0.72	−0.74	0.61	0.57
0.2 spans	−1.56	−1.73	4.02	3.15	−1.67	−1.82
0.5 spans	−0.18	−0.25	0.63	0.45	−0.20	−0.28
1.0 span	0.40	0.38	−0.37	−0.45	0.40	0.39

5. Influence of Initial Stress

5.1. Displacement and Displacement Field. As shown in Figure 11, a fault near mining tunnel divides surrounding rock mass into two regions: one region contains mining tunnel and the other region does not. The continuity of the displacement field of the surrounding rock mass is destroyed by the fault. The displacement field is divided by the fault under the condition where the fault is opened by the excavation load. Comparing with the displacement field of the region with tunnel, the displacement of surrounding rock mass is very little in the region without tunnel. This is because that the seclusion of the fault in surrounding rock mass prevents the excavation load transferring from the excavated surrounding rock mass to the surrounding rock mass without mining tunnel.

When the lateral pressure coefficient k_0 is 0.38, the maximum horizontal displacement of the right sidewall is 1.64 mm, which is approximately the same displacement of fault-free case. When the lateral pressure coefficients k_0 are

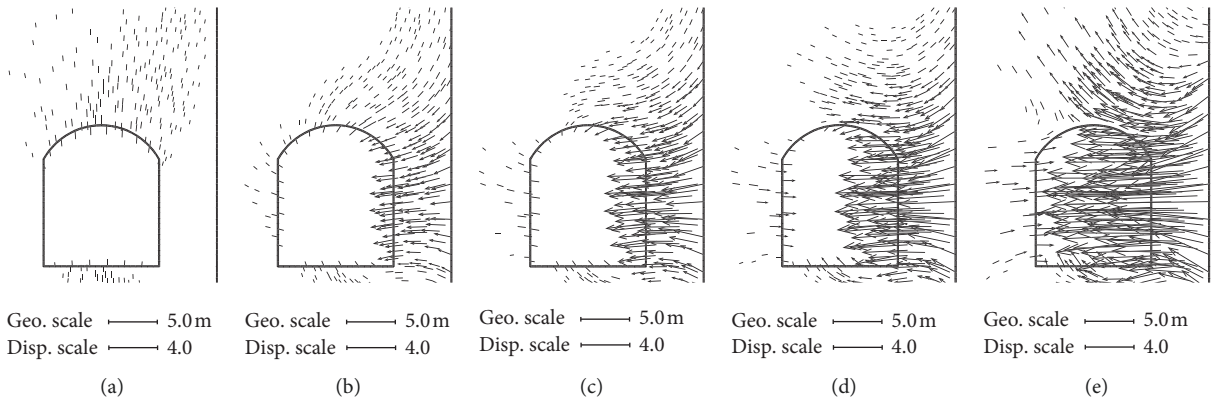

Figure 11: Displacement field of the mining tunnel on five lateral pressure coefficients with right sidewall fault: (a) $k_0 = 0.38$; (b) $k_0 = 1.0$; (c) $k_0 = 1.5$; (d) $k_0 = 2.0$; (e) $k_0 = 3.0$.

1.0, 1.5, 2.0, and 3.0, the maximum horizontal displacements at the right sidewall are 15.9 mm, 28.2 mm, 42.8 mm, and 75.5 mm, respectively, and the displacement ratios λ_d are 1.01, 3.15, 3.56, 3.95, and 4.46, respectively.

For the case with a right sidewall fault and the lateral pressure coefficient greater than 1.0, the maximum displacement near the fault reaches the 3.0–5.0 times that in the fault-free case, whereas the displacement in other region is always less than that in the fault-free case. As shown in Figure 11, the displacement distribution is affected by the lateral pressure coefficient significantly.

5.2. Stress and the Tensile Stress Area of Surrounding Rockmass. The stress vector fields under five different lateral pressure coefficients are plotted in Figure 12. When the lateral stress coefficient is 0.38, the stress vector field is similar to that in the case without fault. With the increasing of horizontal stress, both the lateral stress coefficient and the excavation load on the sidewall increase, which makes the fault close to mining tunnel open significantly. Eventually the tensile stress occurs in the sidewall surrounding rock mass as shown in Figures 12(c)–12(e).

The tensile stress area enlarges with the increasing of the lateral stress coefficient. When the coefficient is 0.38, the tensile stress zone distributes near the mining tunnel crown only. When the coefficient increases to 1.0, the tensile stress expands to the region of the middle of the right wall near the fault. When the lateral stress coefficient increases to 1.5 or 2.0, the tensile stress area enlarges obviously around the right sidewall, and the tensile stress also occurs in the left sidewall zone. The elements with tensile stress are 2, 4, 9, 11, and 17, respectively, corresponding to the lateral stress coefficients of 0.38, 1.0, 1.5, 2.0, and 3.0.

5.3. Plastic Region of Surrounding Rockmass. As shown in Figure 13, the plastic region of the mining tunnel surrounding rock mass is dominated by the fault close to the mining tunnel excavation limit. With the increasing of lateral stress coefficient, the area of plastic region increases dramatically.

Span is a featured geometer parameter for a mining tunnel. The depth of the plastic region is normalized by mining tunnel span in this paper to assess the influence of the initial stress on the plastic region. According to Figure 13, when the lateral stress coefficients are 0.38, 1.0, 1.5, 2.0, and 3.0, the depths of the plastic regions are 0.1, 0.3, 0.4, 0.6, and 0.8 times the mining tunnel span, respectively.

5.4. Inner Force and Stress in Sprayed Concrete Layer. The max stress, i.e., the largest tensile stress in sprayed concrete layer, the min stress, and the largest compressive stress in sprayed concrete layer, are direct indexes to assess the safety status of the sprayed concrete layer in mining tunnel engineering. Two indexes also play a decisive role in the failure or collapse of sprayed concrete layer. The max and min stresses in sprayed concrete layer at key point on the mining tunnel excavation limit are shown in Table 3.

The stress in sprayed concrete layer changes obviously with the lateral stress coefficient. Both the max stress and the min stress increase significantly with the increasing of the lateral stress coefficient, especially the stresses around the right sidewall near a close fault. When the lateral stress coefficient is 0.38, 1.0, and 3.0, the maximum tensile stresses at the midpoint of right sidewall are 0.6, 6.3, and 12.3 MPa, respectively.

6. Field Investigation and Case Study

In Figure 14, a mining tunnel is influenced by a fault F3 at the mining tunnel crown in the section of milestone 0 + 310.15~0 + 380.50. Three across sections A, B, and C are monitored on displacement during the excavation process. The fault distances are 0.2 spans, 0.5 spans, and 1.0 span for sections A, B, and C.

The displacements of the three points (left sidewall midpoint, crown midpoint, and right sidewall midpoint) during excavation are list in Table 4. According to the monitored field displacement, the displacements on the excavation limit have similar characteristics in both the numerical experiment of this work and the field monitoring: the displacement increases with the decreasing of fault

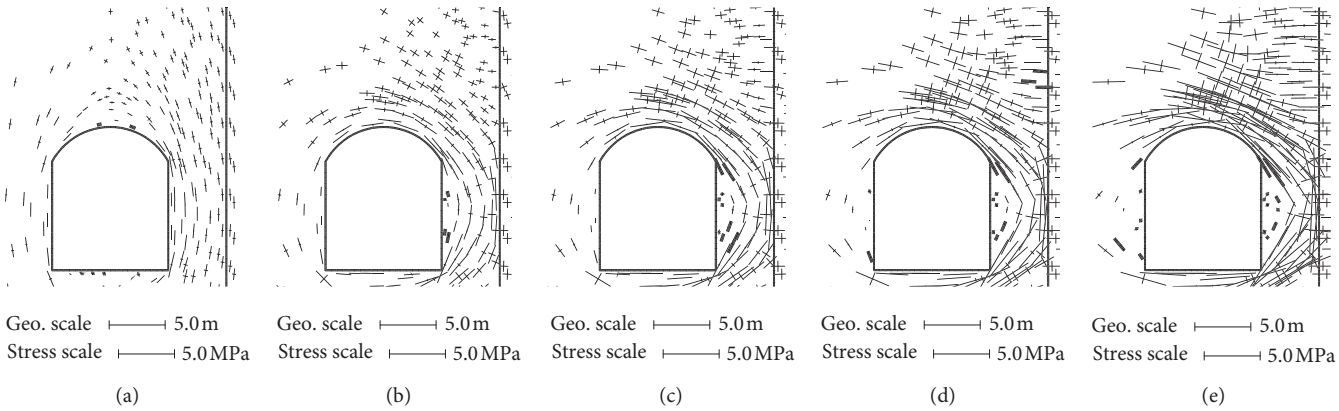

Figure 12: Stress fields under different lateral stress coefficients: (a) $k_0 = 0.38$; (b) $k_0 = 1.0$; (c) $k_0 = 1.5$; (d) $k_0 = 2.0$; (e) $k_0 = 3.0$.

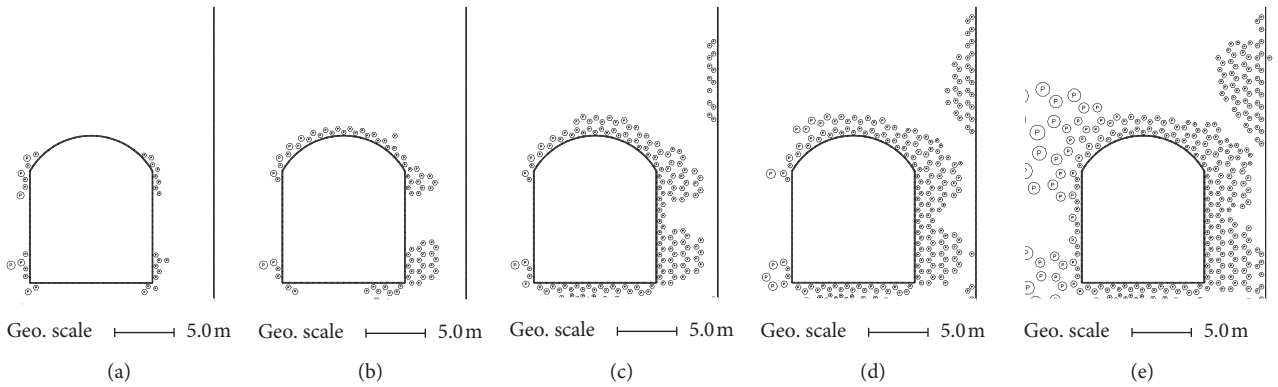

Figure 13: Plastic region at different lateral stress coefficients: (a) $k_0 = 0.38$; (b) $k_0 = 1.0$; (c) $k_0 = 1.5$; (d) $k_0 = 2.0$; (e) $k_0 = 3.0$.

Table 3: The stress of the key point in the sprayed concrete layer.

Lateral stress coefficient k_0	Left sidewall midpoint		Crown midpoint		Right sidewall midpoint	
	σ_{max}	σ_{min}	σ_{max}	σ_{min}	σ_{max}	σ_{min}
0.38	0.6	0.6	−0.7	−0.7	0.6	0.6
1.00	1.3	1.2	−8.3	−8.5	6.3	5.9
1.50	1.8	1.7	−17.0	−17.4	6.8	6.3
2.00	2.3	2.1	−26.4	−26.9	7.7	7.2
3.00	3.4	3.0	−48.2	−49.0	12.3	10.9

Note. − represents compressive stress, whereas tensile stress, unit: MPa.

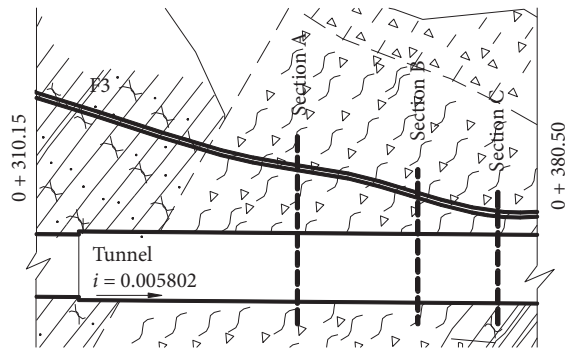

Figure 14: Mining tunnel, F3 fault, and monitoring section.

Table 4: Displacement of the mining tunnel key point during excavation.

Key point	Section A	Section B	Section C
Left sidewall	2.02	2.49	1.87
Crown top	−11.12	−24.54	−48.74
Right sidewall	−2.01	−2.47	−1.85

Note. − represents downward in vertical direction or toward left in horizontal direction, unit: mm.

distance, but the values are doubled in the in-site monitoring comparing to the numerical results.

7. Conclusions

In this paper, a series of numerical experiments were carried out to investigate the influence of fault distance and initial ground stress on the stability of the surrounding rock mass of mining tunnel. The main conclusions are as follows:

(1) Faults with different distances from excavation limit affect apparently the displacement, stress, and plastic region in surrounding rock mass, especially the close fault. There is a critical distance to judge whether a fault has prominent influence, and the critical distance depends on the quality of mining tunnel surrounding rock mass, initial ground stress, and the

curvature degree of excavation limit. When the fault distance is less the critical distance, the displacements of the rock mass between the fault and excavation limit increase dramatically, eventually resulting in the instability of surrounding rock,.

(2) Both the distribution and the value of inner force in the special segment are affected dramatically by fault distance. The axial force in some parts of SCL increases and in some parts decreases as the fault moves from excavation limit (0.2 spans) to deep surrounding rock mass (fault-free).

(3) There are different influence laws at crown and sidewall on displacement of mining tunnel surrounding rock mass regarding to the lateral pressure coefficient in rock stratum. With the increasing of lateral pressure coefficient, the vertical displacement of the crown decreases, but the horizontal displacement of the right sidewall increases.

(4) When the lateral pressure coefficient is 0.38, the tensile stress area equals approximately to that in the fault-free case. When the coefficient is 1.0, the tensile stress area is double that in fault-free case. When the coefficient increases to 2.0 or 3.0, the tensile stress area is 9.0 times that in fault-free case.

(5) When the lateral pressure coefficient is 0.38, there is no difference in the cases with and without fault. When the lateral pressure coefficients are 1.0, 1.5, 2.0, and 3.0, the plastic region doubles comparing with the fault-free case.

(6) When the lateral pressure coefficient is greater than 1.0, the maximum tensile stress in SCL increases sharply comparing with the fault-free case. When the lateral pressure coefficients are 1.0 and 3.0, the tensile stress on the right sidewall are roughly 10 times and 20 times that in the case without fault.

Data Availability

The data used to support the findings of this study are available from the corresponding author upon request.

Conflicts of Interest

The authors declare no conflicts of interest.

Acknowledgments

The scientific research program is supported by the National Natural Science Foundation of China (11872301) and the Shaanxi Provincial Education Department Researching Foundation (17JS091). The author would like to thank Prof. Gunter Swoboda for his suggestions and cooperation in preparing the manuscript.

References

[1] J. A. Hudson and J. P. Harrison, *Engineering Rock Mechanics an Introduction to the Principles (V1)*, Pergamon, London, UK, 2001.

[2] J. A. Hudson, X. T. Feng, and F. Tan, *Rock Characterisation, Modelling and Engineering Design Methods*, CRC Press/Balkema, Taylor & Francis Group, London, UK, 2015.

[3] Z. Zhang, F. Chen, N. Li, G. Swoboda, and N. Liu, "Influence of fault on the surrounding rock stability of a tunnel: location and thickness," *Tunnelling and Underground Space Technology*, vol. 61, pp. 1–11, 2017.

[4] G. Everling, "Model tests concerning the interaction of ground and roof support in gate-roads," *International Journal of Rock Mechanics and Mining Sciences & Geomechanics Abstracts*, vol. 1, no. 3, pp. 319–326, 1964.

[5] D. W. Hobbs, "Scale model studies of strata movement around mine roadways-IV. Roadway shape and size," *International Journal of Rock Mechanics and Mining Sciences & Geomechanics Abstracts*, vol. 6, no. 4, pp. 365–404, 1969.

[6] S. Jeon, J. Kim, Y. Seo, and C. Hong, "Effect of a fault and weak plane on the stability of a tunnel in rock-a scaled model test and numerical analysis," *International Journal of Rock Mechanics and Mining Sciences*, vol. 41, pp. 658–663, 2004.

[7] X. Liu, X. Li, Y. Sang, and L. Lin, "Experimental study on normal fault rupture propagation in loose strata and its impact on mountain tunnels," *Tunnelling and Underground Space Technology*, vol. 49, pp. 417–425, 2015.

[8] N. Li and G. Swoboda, "Discussion on the application of numerical methods to rock mechanics and engineering," *Chinese Journal of Rock Mechanics and Engineering*, vol. 16, no. 5, pp. 502–505, 1997.

[9] G. Bruneau, M. R. Hudyma, J. Hadjigeorgiou, and Y. Potvin, "Influence of faulting on a mine shaft-a case study: part II-numerical modelling," *International Journal of Rock Mechanics and Mining Sciences*, vol. 40, no. 1, pp. 113–125, 2003.

[10] D. Place and P. Mora, "Numerical simulation of localisation phenomena in a fault zone," *Pure and Applied Geophysics*, vol. 157, pp. 1821–1845, 2000.

[11] Z. Q. Zhang, N. Li, F. F. Chen et al., "Influence of weak interbed distributed at different intervals on underground opening stability," *Rock and Soil Mechanics*, vol. 28, no. 7, pp. 1363–1368, 2007.

[12] B. H. Brady and E. T. Brown, *Rock Mechanics: For Underground Mining*, Springer Science & Business Media, Berlin, Germany, 2013.

[13] J. G. Jiang, "Stability of mining tunnel in jointed surrounding rock under different tectonic stress," *Journal of South West JiaoTong University*, vol. 29, no. 1, pp. 20–23, 1982.

[14] M. Bayati and J. Khademi Hamidi, "A case study on TBM tunnelling in fault zones and lessons learned from ground improvement," *Tunnelling and Underground Space Technology*, vol. 63, pp. 162–170, 2017.

[15] G. Swoboda, *Program System Final-Finite Element Analysis Program for Linear and Nonlinear Structures*, University of Innsbruck, Innsbruck, Austria, 1998.

[16] R. E. Goodman, H. E. Heuze, and G. J. Bureau, "One modeling techniques for the study of mining tunnel in jointed rock," in *Proceedings of the 14th U.S. Symposium on Rock Mechanics*, pp. 441–479, University Park, PA, USA, June 1972.

[17] C. S. Desai, M. M. Zaman, J. G. Lightner, and H. J. Siriwardane, "Thin-layer element for interfaces and joints," *International Journal for Numerical and Analytical Methods in Geomechanics*, vol. 8, no. 1, pp. 19–43, 1984.

[18] G. Swoboda and M. Marence, "Numerical modelling of rock bolts in intersection with fault system," in *Numerical Models in Geomechanics*, G. N. Pande and S. Pietruszczak, Eds., pp. 729–738, Balkema, Rotterdam, Netherlands, 1992.

[19] S. Sakurai and K. Takeuchi, "Back analysis of measured displacements of tunnels," *Rock Mechanics and Rock Engineering*, vol. 16, no. 3, pp. 173–180, 1983.
[20] Z. Q. Zhang, N. Li, F. F. Chen et al., "Influence of weak interbed on stability and safety of underground at different confining pressure environment," *Journal of Hydroelectric Engineering*, vol. 28, no. 2, pp. 78–83, 2009.
[21] C. Fairhurst, "Stress estimation in rock: a brief history and review," *International Journal of Rock Mechanics and Mining Sciences*, vol. 40, no. 7-8, pp. 957–973, 2003.
[22] R. E. Goodman, R. L. Taylor, and T. L. Brekke, "A model for the mechanics of jointed rock," *Journal of the Soil Mechanics and Foundations Division*, vol. 99, pp. 637–660, 1968.
[23] B. Amadei and O. Stephansson, *Rock Stress and Its Measurement*, Chapman & Hall, London, UK, 1997.
[24] P. Jia and C. A. Tang, "Numerical study on failure mechanism of tunnel in jointed rock mass," *Tunnelling and Underground Space Technology*, vol. 23, no. 5, pp. 500–507, 2008.